Human Pathology (2012) **43**, 197–208

ELSEVIER

Human PATHOLOGY

www.elsevier.com/locate/humpath

Original contribution

Metallothionein expression in colorectal cancer: relevance of different isoforms for tumor progression and patient survival☆

Juan Martín Arriaga MSc[a], Estrella Mariel Levy PhD[a], Alicia Inés Bravo MD[b], Sergio Morales Bayo MD[c], Mora Amat MD[d], Mariana Aris MSc[e], Adrián Hannois MD[b], Luisina Bruno MD[d], María Paula Roberti MSc[a], Fernando Sánchez Loria MD[d], Alejandro Pairola MD[d], Eduardo Huertas MD[d], José Mordoh MD, PhD[a,d,e], Michele Bianchini PhD[a,*]

[a]*Centro de Investigaciones Oncológicas de la Fundación Cáncer, 1426 Buenos Aires, Argentina*
[b]*Hospital Interzonal General de Agudos Eva Perón. 1650 San Martín, Argentina*
[c]*Hospital Municipal Prof. Dr Houssay, 1638 Vicente López, Argentina*
[d]*Instituto Médico Especializado Alexander Fleming, 1426 Buenos Aires, Argentina*
[e]*Instituto de Investigaciones Bioquímicas de Buenos Aires, IIBBA CONICET, Fundación Instituto Leloir, 1405 Buenos Aires, Argentina*

Received 30 March 2011; revised 15 April 2011; accepted 22 April 2011

Keywords:
Metallothioneins;
Colorectal cancer;
Biomarker;
Oncogenesis;
Hypermethylation;
Survival

Summary Metallothioneins are a family of small, cysteine-rich proteins with many functions. Immunohistochemical evaluation of all metallothionein 1 + 2 isoforms in colorectal tumors has demonstrated an important down-regulation compared with normal tissue, although its prognostic significance is unclear. Moreover, the contribution of individual isoforms to overall metallothionein down-regulation is not known. To address these important issues, we analyzed the messenger RNA expression levels of all functional metallothionein 1 + 2 isoforms by quantitative reverse transcription polymerase chain reaction in 22 pairs of normal and tumor-microdissected epithelia and correlated these to the overall immunohistochemical protein expression. Our results showed that 5 isoforms (MT1G, 1E, 1F, 1H, and 1M) were lost during the transition from normal mucosa to tumor, whereas MT1X and MT2A were less down-regulated, and their expression was correlated with overall protein positivity. Second, we showed that *MT1G* hypermethylation occurred in cell lines and in 29% of tumor samples, whereas histone deacetylase inhibitors are able to induce most isoforms. Furthermore, we analyzed by immunohistochemistry 107 normal mucosae, 25 adenomas, 81 carcinomas, and 19 lymph node metastases to evaluate metallothionein expression during different stages of cancer development and to assess its relationship to patient survival. A lower immunohistochemical expression was associated with

Abbreviations: AFC, average fold change; CI, confidence interval; CRC, colorectal cancer; DAC, 5-aza-2′-deoxycytidine; HDACs, histone deacetylases; HR, hazard ratio; IHC, immunohistochemistry; MSP, methylation-specific PCR; MT, metallothionein.

☆ This work was funded by Fundación Cáncer, Consejo Nacional de Investigaciones Científicas y Técnicas (CONICET) (PIP No. 845-10), ANPCyT, Fundación P. Mosoteguy, Fundación Sales, and Fundación María Calderón de la Barca. M.B., J.M., and E.M.L. are members of CONICET, and J.M.A., M.A., and M.P.R. are fellows of the same institution.

* Corresponding author. Instituto Médico Especializado "Alexander Fleming," Zabala 2836, 1426 Buenos Aires, Argentina.
E-mail address: mbianchini@conicet.gov.ar (M. Bianchini).

0046-8177/$ – see front matter
doi:10.1016/j.humpath.2011.04.015

poorer survival, although it was not an independent predictor. Overall, this study identifies for the first time the relevant metallothionein isoforms for colorectal cancer progression, supports the concept that their loss is associated with worse prognosis, and suggests 2 mechanisms for epigenetic repression of metallothionein expression in colorectal tumors.

1. Introduction

Metallothioneins (MTs) constitute a superfamily of nonenzymatic, low-molecular-weight (6-7 kd) proteins, characterized by a distinctive amino acid composition: high cysteine content (30%), no aromatic amino acids, and no, or low, histidine. In humans, there are at least 11 functional MT genes that are divided into 4 subgroups (MT1-4) and clustered within an 82.1-kb region on chromosome 16q13 [1]. The MT-1 isoforms and MT-2A are ubiquitously expressed and are the most extensively characterized MTs. They are rapidly induced by a wide variety of agents including inflammatory cytokines, hormones, and cytotoxic agents. Although the primary role of MTs is controversial, they are known to regulate Zn^{2+} homeostasis and to be involved in cellular defense mechanisms such as protection against nonessential heavy metals and oxidizing agents [2,3]. Because Zn^{2+} is associated with more than 300 proteins that function in metabolism, gene expression, and cell growth, by supplying or removing Zn^{2+}, MTs can activate or inactivate various Zn-binding proteins [4,5] and thus regulate a wide variety of cellular processes.

MT expression in colorectal cancer (CRC) has been studied by radioimmunoassay and immunohistochemistry (IHC) using antibodies that recognize isoforms 1 and 2 and shown to be progressively down-regulated during CRC progression [6,7]. Although the prognostic significance of MT expression in CRC has not been clearly defined, several studies agree that tumors with lower MT expression have worse prognosis [8]. At the messenger RNA (mRNA) level, different MT1 + 2 isoforms have been studied using complementary DNA (cDNA) microarray expression profiling [9,10]. Using this methodology [11], our group has previously reported that the fourth most down-regulated gene in CRC at the transcript level was MT1G (in 18 of 19 tumors), whereas MT1H, MT1F, and MT2A were down-regulated in at least 15 of 19 samples. Despite this, no study has until now specifically analyzed the expression of all MT functional isoforms or attempted to correlate this with MT1 + 2 protein expression.

2. Materials and methods

2.1. Patients and tissue samples

A total of 81 patients (mean age, 69 years; range, 49-89 years) from 2 different hospitals (Instituto Alexander Fleming and Hospital Houssay) were submitted to surgery for histologically proven adenocarcinoma of the colorectum. For 22 of these, both tumor and morphologically normal mucosa (taken more than 5 cm away from the tumor) were split into RNA Later medium (Ambion Inc., Austin, TX) or 4% formalin, for subsequent RNA and immunohistochemical analyses, respectively. RNA Later–preserved tissues were left at 4°C for 24 hours and then stored at −80°C. For the rest of the carcinomas and for 25 adenomas and 17 mucosae from nononcologic patients, tissues were routinely processed in 4% formalin and embedded in paraffin blocks. This research was approved by the institutional review boards of both institutions.

2.2. Cell lines and treatment

Five CRC cell lines were obtained from the American Tissue Culture Collection: HCT-116, CACO-2, HT-29, DLD-1, and T84. All cell lines were grown at 37°C in a humid atmosphere containing 5% CO_2 with Dulbecco modified Eagle medium (Invitrogen, San Diego, CA), supplemented with 10% heat-inactivated fetal calf serum, 2 mmol/L L-glutamine, 3.5 mg/mL sodium carbonate, and 4.5 mg/mL glucose. For 15 μmol/L 5-aza-2′-deoxycytidine (DAC; Sigma-Aldrich Inc, St Louis, MO) and 500 ng/mL Trichostatin A (TSA; InvivoGen, San Diego, CA) treatments, 5×10^4 cells were plated in 24 multiwell plates and treated for 72 hours (renewed every 24 hours) and 24 hours, respectively.

2.3. RNA extraction and cDNA preparation

RNA Later–preserved tissues were fixed in methacarn (60% methanol, 30% chloroform, 10% acetic acid) for 2 hours, dehydrated in a series of graded alcohols and embedded in paraffin blocks. Ten-micrometer-thick sections were subsequently obtained using a microtome and stained with crystal violet. Normal and tumor epithelia were laser capture microdissected (Leica AS LMD; Leica Microsystems, Wetzlar, Germany) and recovered in 20 μL of lysis buffer for total RNA extraction (RNAqueous-Micro Kit; Ambion Inc, Austin, TX). Finally, RNA was reverse transcribed using the Moloney Murine Leukemia Virus Reverse Transcriptase (M-MLV RT) (Invitrogen).

2.4. Genomic DNA extraction and bisulfite treatment

Genomic DNA from microdissected samples and colorectal cell lines was isolated, and the resulting DNA was treated with

bisulfite to convert unmethylated cytosines to uracil, using the EZ DNA Methylation-Direct Kit (Zymo Research, Orange, CA). To determine *MT1G* promoter methylation levels, we designed primers for methylation-specific polymerase chain reaction (PCR), or MSP, analysis [12] that specifically recognize the methylated (M) and unmethylated (U) regions of the *MT1G* promoter (Supplementary Table 1). CRC cell lines were used as positive or negative controls for both pairs of primers. MSP analysis was carried out using 0.5 μg of bisulfate-converted DNA, and methylation levels were calculated using the M/U ratio. For surgical samples, the $\Delta\Delta C_t$ method was used to compare the expression in tumor against paired normal tissue, and cases showing positive ratios were called methylated. For cell lines, the M/U ratio was used to compare methylation levels between the different lines.

2.5. Real-time PCR and MSP

Real-time PCR analysis was performed using the set of primers reported in Supplementary Table 1. The MT isoform primers were designed to target UTR regions of the cDNA, where the transcripts show less homology to each other. PCR runs were carried out using SYBR Universal Master Mix (Applied Biosystems, Carlsbad, CA), and relative expression levels were determined by the $\Delta\Delta C_t$ method using β-actin gene expression to normalize all samples. Both melting curve analysis and gel electrophoresis assessment were used to confirm the specificity of PCR reactions. Amplification efficiency, linearity of the dynamic range, and the sensitivity limit were estimated for each pair of primers by standard curve calculation derived from serial dilutions of positive cDNA obtained from CRC cell lines (Supplementary Table 1). PCR reactions were corrected for the different efficiencies so that expression levels could also be compared between isoforms.

2.6. Immunohistochemistry

Immunohistochemical analysis of MT protein expression was done using the monoclonal mouse anti-MT clone E9 antibody (Dako Corporation, Carpinteria, CA), dilution 1:150, which recognizes all MT1 + 2 isoforms. Antigen retrieval was done by heating slides immersed in citrate buffer pH 6.0 in a microwave oven (95-100°C) for 2 rounds of 10 minutes each. Given that some authors report that antigen retrieval is not necessary for MT detection using E9 antibody, it is worth mentioning that this procedure did enhance MT positivity in our tissues (data not shown). Detection was carried out using the Vectastain Universal Elite ABC kit (Vector Labs, Burlingame, CA) as instructed by the manufacturer, with DAB as substrate. Slides were then counterstained in 1:5 hematoxylin solution, dehydrated, and mounted in Canada Balsam synthetic. MT staining was scored using the immunoreactivity score (IRS) scale [13], which grades positivity in a scale from 0 to 12 that results from multiplying the percentage positivity score (0-4) by the intensity score (0-3). Percentage score was defined as 0 if less than 1% of cells were positive, 1 if 1% to 10%, 2 if 11% to 50%, 3 if 51% to 80%, and 4 when more than 80% of cells stained positively. Intensity was scored 0 for negative staining, 1 for barely detectable stain, 2 if positivity could be easily detected using high-powered magnification (×200), and 3 if low-powered magnification allowed clear signal detection. Next, for analytical purposes, IRS scores were grouped into 4 positivity groups: IRS score 0 was called "–"; 1 to 3, "+"; 4 to 8, "++"; and 9 to 12, "+++."

2.7. Western blotting and immunofluorescence

MT1 + 2 protein quantification in cell lines was carried out using Western blotting. Briefly, cells were lysed in radioimmunoprecipitation assay (RIPA) buffer, protein concentrations determined by the Bradford method, and 70 μg of total protein electrophoresed in 15% sodium dodecyl sulfate–polyacrylamide gel electrophoresis and transferred onto nitrocellulose membranes at 300 mA for 1 hour. Membranes were fixed in 2.5% glutaraldehyde, washed twice in phosphate-buffered saline (PBS) and once in PBS-50 mmol/L monoethanolamine, and then blocked overnight at 4°C in 2.5% skim milk in PBS-Tween (PBST) 0.01%. Immunodetection was done with E9 antibody (1:1000) for 1 hour, peroxidase horse antimouse immunoglobulin G antibody (Vector), and signal detection with electrochemical luminescence (Pierce Biotechnology, Rockford, IL). β-Actin levels were used as loading controls, using mouse monoclonal anti–β-actin, clone AC-74 (Sigma). For immunofluorescence labeling, cell lines were plated onto glass coverslips, fixed in 3% paraformaldehyde for 30 minutes, washed 3 times in PBS, permeabilized in 0.4% Triton X-100 in PBS for 10 minutes, washed 3 times, blocked in PBS-bovine serum albumin (BSA) 10% for 30 minutes, and incubated overnight at 4°C with E9 antibody, 1:100 dilution in 3% BSA 0.4% Triton-PBS. Next, after 3 washes in PBST, 0.5% slides were incubated for 2 hours with phycoerythrin conjugated goat antimouse polyclonal antibody (Dako), diluted 1:50 in 3% BSA 0.4% Triton-PBS; then washed again in PBST; counterstained with Hoechst 5 μg/mL; and finally fixed in 1% paraformaldehyde before mounting in Mowiol (Merck KGaA, Darmstadt, Germany) and observed under a fluorescence microscope.

2.8. Patient follow-up and statistical analysis

Student t test and χ^2 test were used to assess means and distributions, respectively. MT isoform levels between different patient groups were assessed by analysis of variance and the paired Student t test (thus eliminating possible variations in mRNA expression between different patients), whereas mRNA and protein levels were correlated using Pearson correlation analysis. Eighty-one patients were selected for survival analysis based on the availability of follow-up, which was concluded in October 2010. None of these patients

died within 30 days after surgery. Median follow-up time (as evaluated by the reverse Kaplan-Meier method) was 51.3 months. Twenty-seven patients died, 40 were still alive, and 14 were lost during the follow-up period. All-cause mortality was used as end point for overall survival (OS), and disease-free survival (DFS) was estimated using relapse or death as events, whichever occurred first. The cumulative patient survival was estimated using the Kaplan-Meier method, and for univariate survival analysis, the log-rank test was used. The Cox proportional hazards linear regression model was used for multivariate analysis in a backward stepwise procedure. *P* values less than .05 were considered significant. GraphPad Prism (La Jolla, CA) and MedCalc (Mariakerke, Belgium) softwares were used for analysis.

3. Results

3.1. MT isoforms expression analysis by quantitative real-time PCR in microdissected epithelial colon cells from surgical samples

The main goals of this study were to validate our microarray results [11] using quantitative reverse transcriptase PCR (qRT-PCR) and to investigate the expression of all the functional MT variants in cancer cells relative to their normal counterparts. We used total RNA from laser capture microdissected pure cell (~100%) populations and determined the mRNA expression ratios of the 9 functional MT-1 and MT-2A isoforms in 45 samples from 22 patients with CRC (2 with Dukes A, 10 with Dukes B, 8 with Dukes C, 2 with Dukes D, and 1 matched liver metastasis), using specific primers for each gene (shown in Supplementary Table 2). The β-actin mRNA expression was used as reference for normalization. Informative results (based on expression level and/or reproducibility) were obtained for all isoforms except for MT1B, confirming its limited tissue expression.

We observed that MT1E, MT1M, MT1X, and MT2A were the most highly expressed isoforms in tumor epithelia, whereas the expression level of MT1A, MT1F, MT1G, and MT1H was significantly lower (Tukey multiple comparison test, $P < .05$; Fig. 1A). In normal mucosae, we did not observe significant differences in the absolute amount of different MT isoforms except for MT1E, whose expression was significantly higher than the rest ($P < .05$; data not shown).

The $\Delta\Delta C_t$ method was used to compare expression levels between tumor and paired normal cells. Tumor samples with an expression level half that of matched normal mucosae (average fold change, <-2) were called down-regulated, and their frequencies are reported in Table 1. MT down-regulation occurred in 57% to 91% of the cases analyzed, depending on the isoform (Table 1). MT1E, MT1G, and MT1F were the most repressed isoforms, whereas MT1X and MT2A failed to reach statistical significance ($P > .05$; Fig. 1B). It is noteworthy that in the only hepatic metastasis studied, the expression levels of all isoforms were the same as those in the primary tumor (Supplementary Table 2).

3.2. Validation of MT1 + 2 down-regulation by IHC and correlation with isoform expression

We examined the overall MT expression by IHC in the same 22 patients, using the E9 monoclonal antibody that recognizes all MT1 + 2 isoforms. MT staining was grouped into 4 categories: −, +, ++, and +++, as explained in the "Materials and Methods" section. Protein down-regulation occurred in 18 (82%) of 22 cases, confirming the results obtained at the mRNA level. Interestingly, in the 4 tumors that scored +++ (showing expression levels similar to normal mucosae), some isoforms showed mRNA down-regulation. To determine which isoforms were responsible for MT protein expression in tumors, we correlated the IHC staining scores (as evaluated with the 0-12 grade IRS scale) with the mRNA expression levels of all isoforms. Pearson correlation analysis demonstrated a significant positive correlation only for MT2A (Pearson $r = 0.47$ $P = .03$) and MT1X (Pearson $r = 0.61$ $P = .004$).

3.3. MT isoforms mRNA and protein expression in 5 colorectal cell lines

To evaluate MTs expression in the in vitro setting, we studied their mRNA levels by qRT-PCR in HCT-116, DLD-1, HT-29, CACO-2, and T84 cell lines. Although all isoforms (except MT1B) could be detected, MT1E, MT2A, and MT1X were the most abundant in all cell lines except T84, which expressed all variants just above their detection limit (data not shown). Next, we quantified MT protein expression by Western blotting and analyzed its subcellular localization by immunofluorescence. As shown in Fig. 2, these cell lines expressed variable amounts of MT protein (Fig. 2A), with different subcellular localization (nuclear or cytoplasmatic; Fig. 2B). T84 cells expressed undetectable protein levels. MT2A was the only isoform whose mRNA levels correlated significantly to protein levels as determined by Western blotting (Pearson $r = 0.96$, $P = .009$).

3.4. MSP of CRC surgical samples and cell lines

Sequence analyses of the regions approximately 1 kb upstream from the transcription start site of the *MT1G* gene revealed numerous CpG sites, which are potential targets for DNA methylation. To investigate the possibility that MT1G expression is regulated by promoter hypermethylation, we conducted MSP analysis on 14 human clinical samples using bisulfite-converted DNA from microdissected tumor and normal colorectal cells. Methylation levels were expressed as the methylated/unmethylated ratio using the ΔΔCt method. In 4 (29%) of 14 cases, promoter methylation was higher in the tumor than in the corresponding noncancerous

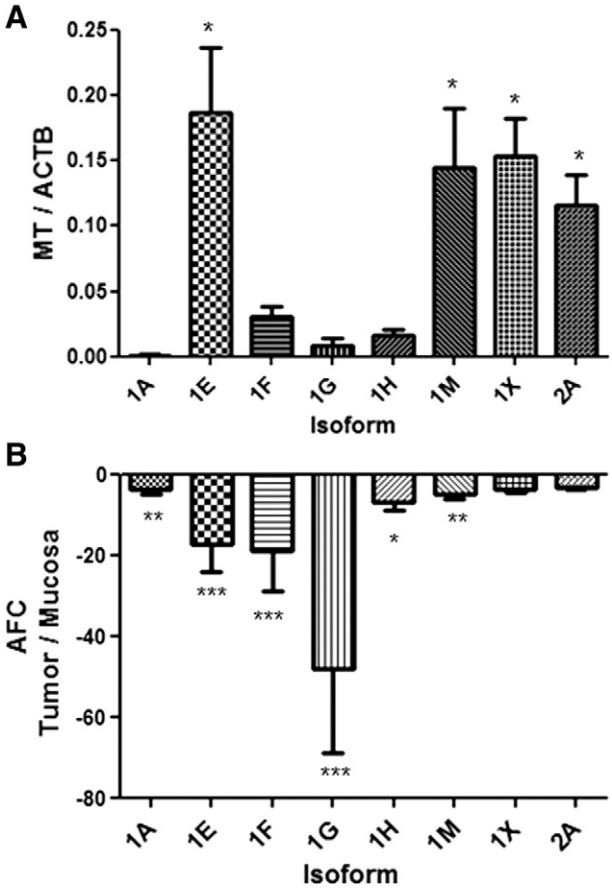

Fig. 1 Histogram plots showing MT isoforms mRNA expression levels measured by qRT-PCR. A, MT tumor expression levels relative to the β-actin gene. Tumors mainly express MT1E, MT1M, MT1X, and MT2A isoforms, although at lower levels than normal colorectal cells (data not shown). B, Average fold change (AFC) of the different MT isoforms in 22 tumors compared with paired normal tissue, as measured by the $\Delta\Delta C_t$ method. MT1G is the most down-regulated MT transcript, followed by MT1E and MT1F. *P < .05; **P < .01; ***P < .001 (analysis of variance, with Tukey as post test). Data presented as mean ± SEM.

epithelium (Table 2). Remarkably, methylation levels were independent from MT1 + 2 protein levels, indicating that MT1G is regulated differently from other isoforms.

In vitro, HCT-116 and DLD-1 cell lines were classified as MT1G negative because transcript amounts were below the detection limit of qRT-PCR, whereas the other 3 cell lines (T84, CACO2, and HT-29) were classified as MT1G positive. In MSP analysis, promoter methylation levels were significantly higher in HCT-116 and DLD-1 cells than in T84, CACO-2, and HT-29 cell lines (P < .05), faithfully corresponding to the MT1G-negative and MT1G-positive cells, respectively.

To confirm that promoter hypermethylation is functionally relevant in repressing the *MT1G* gene, we examined its mRNA expression after 5-aza-dC (DAC) treatment in 2 CRC cell lines: HCT-116 (methylated) and HT-29 (unmethylated). Treatment with this DNA methyl-transferase inhibitor led to a strong reactivation (750-fold) of MT1G mRNA expression in the HCT-116 cell line, but not in HT-29 (Fig. 3A, B). Analyzing the effect on the other MT isoforms, we suggest that *MT1A* and *MT1H* may also be methylated in HCT-116 cell line.

To test whether other epigenetic mechanisms may regulate MT expression in CRC, we treated these same cell lines with TSA, a potent HDAC inhibitor. Interestingly, we observed a general up-regulation of most MT isoforms in both cell lines, suggesting that HDACs regulate MTs in a more general, nonspecific manner than promoter hypermethylation (Fig. 3C, D).

Table 1 MTs mRNA down-regulation in tumor vs normal tissue

Isoform	Down-regulation level, AFC (M/T) [a]	Down-regulation, frequency (%)	P value (paired t test)
MT1A	3.7	59	.0028
MT1E	17.3	78	.0001
MT1F	18.2	78	.0002
MT1G	46.7	91	.0001
MT1H	6.6	74	.0137
MT1M	4.6	57	.0048
MT1X	3.7	65	.0584
MT2A	3.2	70	.0654

[a] AFC M/T: average fold change (AFC) expressed as the mRNA expression ratio of normal mucosa (M) versus tumor (T).

3.5. MT protein expression by IHC in formalin-fixed surgical samples from normal, adenomatous, primary carcinoma, and metastatic colorectal tissues

We next evaluated MT IHC expression in different stages of CRC development, using a series of normal, adenomatous, carcinomatous, and metastatic human colorectal surgical samples. Staining score frequencies are reported in Table 3.

We first analyzed 17 normal mucosae from patients without CRC ("non-CRC mucosa" in Table 3); we found that epithelial cells were always highly positive, indicating that MT expression is generally abundant in normal epithelium. This was also true in mucosae of 36 patients with colon carcinoma, taken more than 5 cm away from the tumor ("CRC far mucosa"), as well as in 54 tumor-adjacent normal-appearing tissues ("CRC adjacent mucosa"). No significant differences were noted in staining positivity of the different normal samples studied (Table 3). In most cases, epithelial cells stained uniformly strong all along the crypts (Fig. 4A), although the top third of the crypt sometimes stained negatively. Interestingly, the lowermost layer of cells in the crypt usually stained negatively (Fig. 4B). Subcellular localization was nuclear and cytoplasmatic. Nonepithelial cells such as peripheral nerves, smooth muscle, and some endothelial cells also stained positive.

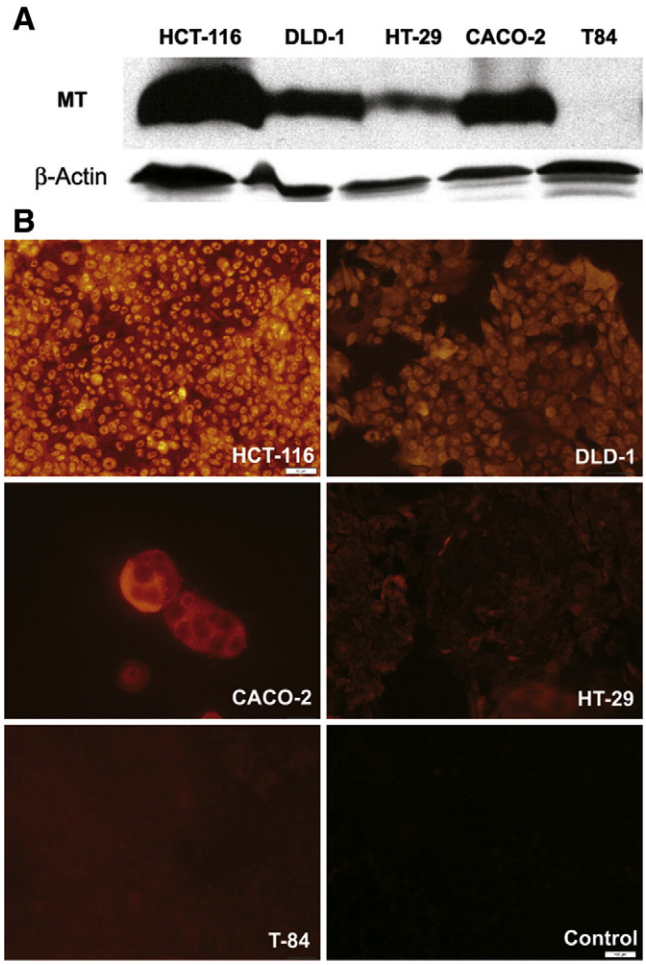

Fig. 2 MT1 + 2 protein expression in CRC cell lines. A, Western blotting shows variable levels of MT expression in the 5 cell lines studied, ranging from high in HCT-116 to null in T84. B, Immunofluorescence staining shows that nuclear and cytoplasmatic localization is found in HCT-116 and DLD-1 cells (original magnification ×200), whereas CACO-2 and HT-29 show only cytoplasmatic expression (for CACO-2, original magnification ×400); no staining was detected in the T84 cell line or in the control slides, devoid of primary antibody.

We then studied 25 adenoma samples, all of which showed constant but heterogeneous positivity, frequently limited to the basal more normal-appearing glandular portions (Fig. 4C). It was very interesting to note in these tissues that dysplastic glands adjacent to normal-appearing glands stained negatively, whereas the latter remained positive (Fig. 4D, E). Overall, MT staining levels were significantly lower in adenomas than in normal tissues (χ^2 test, $P < .0001$). Because adenocarcinomas are thought to arise from adenomas through a stepwise series of changes, our results suggest that MT down-regulation begins early during colon carcinogenesis.

About one third (30 of 81, or 37%) of the colorectal carcinomas investigated completely lacked immunohistochemically detectable MT (as in Fig. 4F), and 28 (35%) of 81 showed very low levels of MT staining. Immunoreactivity in the remaining cases was mainly located in the cytoplasm and nucleus. Most frequently, tumor positivity was very heterogeneous, with positive cells and glands coexisting with adjacent negative ones (Fig. 4G). Only 5% of the tumors studied showed high MT levels, comparable with those of normal mucosae (Fig. 4H).

Finally, we assessed 19 lymph node metastasis samples from some of the patients whose primary tumors had been studied and also observed low levels of MT staining, comparable with primary tumor levels and significantly lower than normal samples (χ^2 test, $P < .0001$; Fig. 4I). Importantly, immunoreactivity was concordant with the corresponding primary tumor in 78% of cases.

Table 2 MSP analysis on human clinical samples

Sample no.	Tumor methylation ratio (T/M) [a]	MT1G down-regulation (AFC M/T) [b]
1	0.04	4.3
2	0.05	14.5
3	0.07	31.5
4	0.08	NA
5	0.15	37.7
6	0.25	6.5
7	0.31	44.3
8	0.38	9.6
9	0.41	44.8
10	0.44	57.8
11	14.36	10.1
12	20.23	20.7
13	114.56	319.0
14	297.00	NA

Abbreviation: NA, not available.
[a] Methylated/unmethylated ratio in tumor (T) vs normal mucosa (M).
[b] AFC M/T: average fold change (AFC) expressed as the mRNA expression ratio of normal mucosae (M) versus tumor (T).

3.6. Relationship between clinicopathologic findings and MT expression

To determine the prognostic significance of MTs in CRC, we evaluated their association with patient survival and standard histoclinical parameters (Table 4). Kaplan-Meier analysis revealed that low MT expression was significantly associated with worse patient survival. Fig. 5 (A, B) shows that a gradual decrease in MT score was significantly associated with a progressive shortening of OS and DFS (log-rank test for trend: $P = .03$ and $P = .02$, respectively). Grouping all positive scores ("+, ++, and +++") against totally negative cases ("−") enhanced the statistical significance in both DFS (log-rank test, $P = .007$; hazard ratio [HR], 2.84; 95% confidence interval [CI], 1.34-6.04; Fig. 5C) and OS (data not shown). Median DFS times were 28.6 months for negative cases and 96 months for all positive groups. When analyzing Dukes stages individually, negative

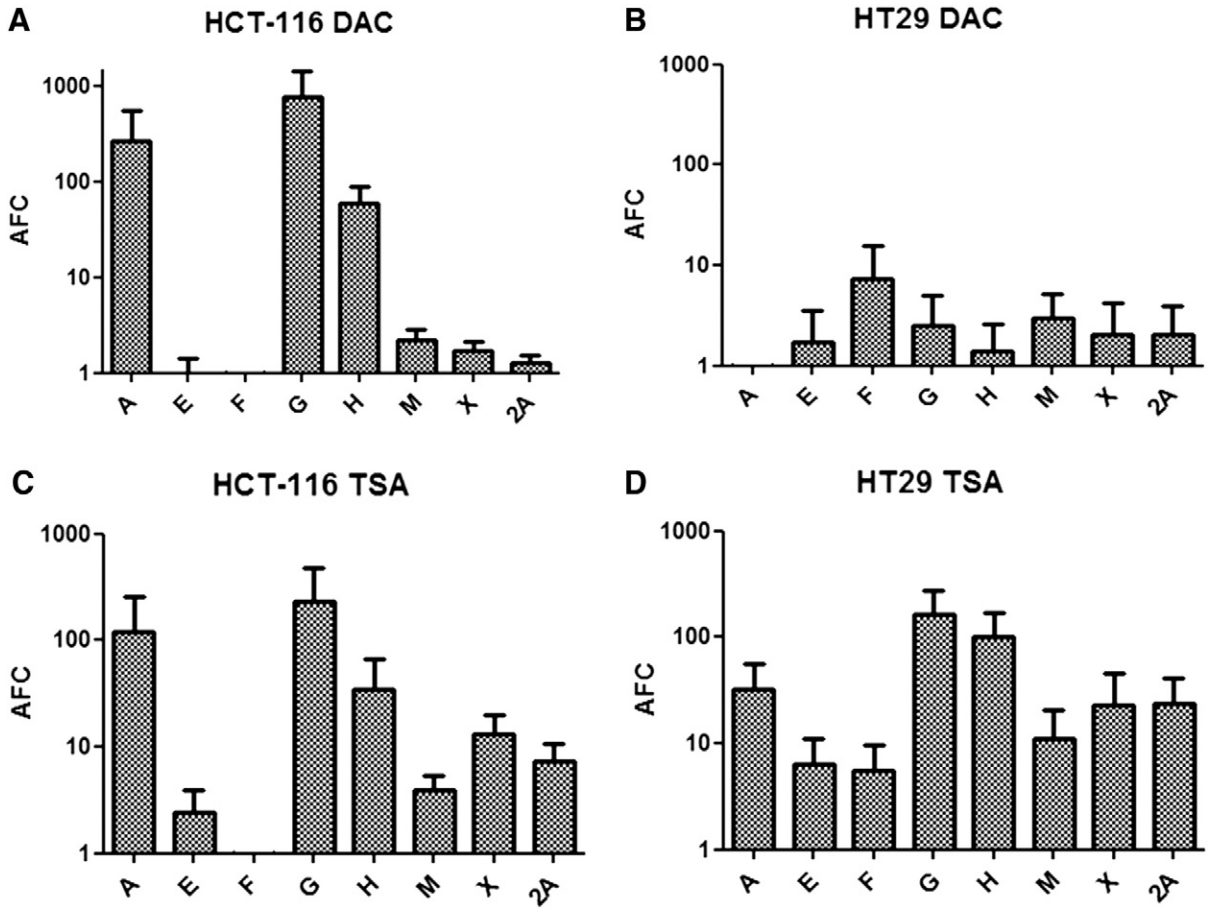

Fig. 3 MTs mRNA up-regulation in cell lines treated with DAC or TSA. A and B, DAC treatment greatly enhances the expression of MT1G, MT1A, and MT1H isoforms in the HCT-116 cell line, whereas the increase is irrelevant in HT-29. This agrees with our observation by MSP analysis that *MT1G* promoter is hypermethylated in the former but not in the latter cell line. C and D, In both cell lines, TSA treatment up-regulates MT isoforms in a more unspecific manner than promoter hypermethylation. Data presented as mean ± SD.

MT staining showed a trend in association with shorter DFS in Dukes B cases (log-rank test, P = .08; HR, 3.98; 95% CI, 0.81-19.46; Fig. 5D) but not in Dukes C. Univariate analysis of standard histoclinical parameters revealed that Dukes, pT (tumor spread), pN (lymph node status), and M (distant metastasis) stages were also associated with OS and DFS (Table 5). However, multivariate analysis by Cox proportional hazards regression, including all covariates shown in Table 5, revealed Dukes stage and mucinous histology as independent predictors of OS (for Dukes: P = .0006; HR, 5.5; 95% CI, 2.1-14.4; for histology: P = .02; HR, 9.6; 95% CI, 1.5-63.4) and DFS (for Dukes: P = .0001; HR, 6.6; 95% CI, 2.6-16.4; for histology: P = .02; HR, 5.6; 95% CI, 1.3-23.7).

Totally negative staining frequency increased with increasing Dukes stage, representing 25% of stage A samples, 31% of stage B, 39% of stage C, and 60% of stage D (Tables 3 and 4), although this trend was not statistically significant. No associations were found between MT staining and routine histopathologic parameters (Table 4).

Table 3 MT1 + 2 staining positivity in colorectal tissues

Samples	n	MT1 + 2 staining scores (% cases)				χ^2 test[a]
		−	+	++	+++	
Non-CRC mucosa	17	0	0	12	88	NS
CRC far mucosa	36	0	3	14	83	
CRC adjacent mucosa	54	0	9	17	74	NS
Adenoma	25	32	32	28	8	P < .0001
Low grade	12	33	25	25	17	
High grade	13	31	38	31	0	
Adenocarcinoma	81	37	35	22	6	P < .0001
Dukes A	4	25	0	50	25	
Dukes B	36	31	33	28	8	
Dukes C	31	39	42	16	3	
Dukes D	10	60	30	10	0	
Lymph node metastasis	19	58	32	10	0	P < .0001

Abbreviation: NS, not significant.
[a] Compared with CRC far mucosa.

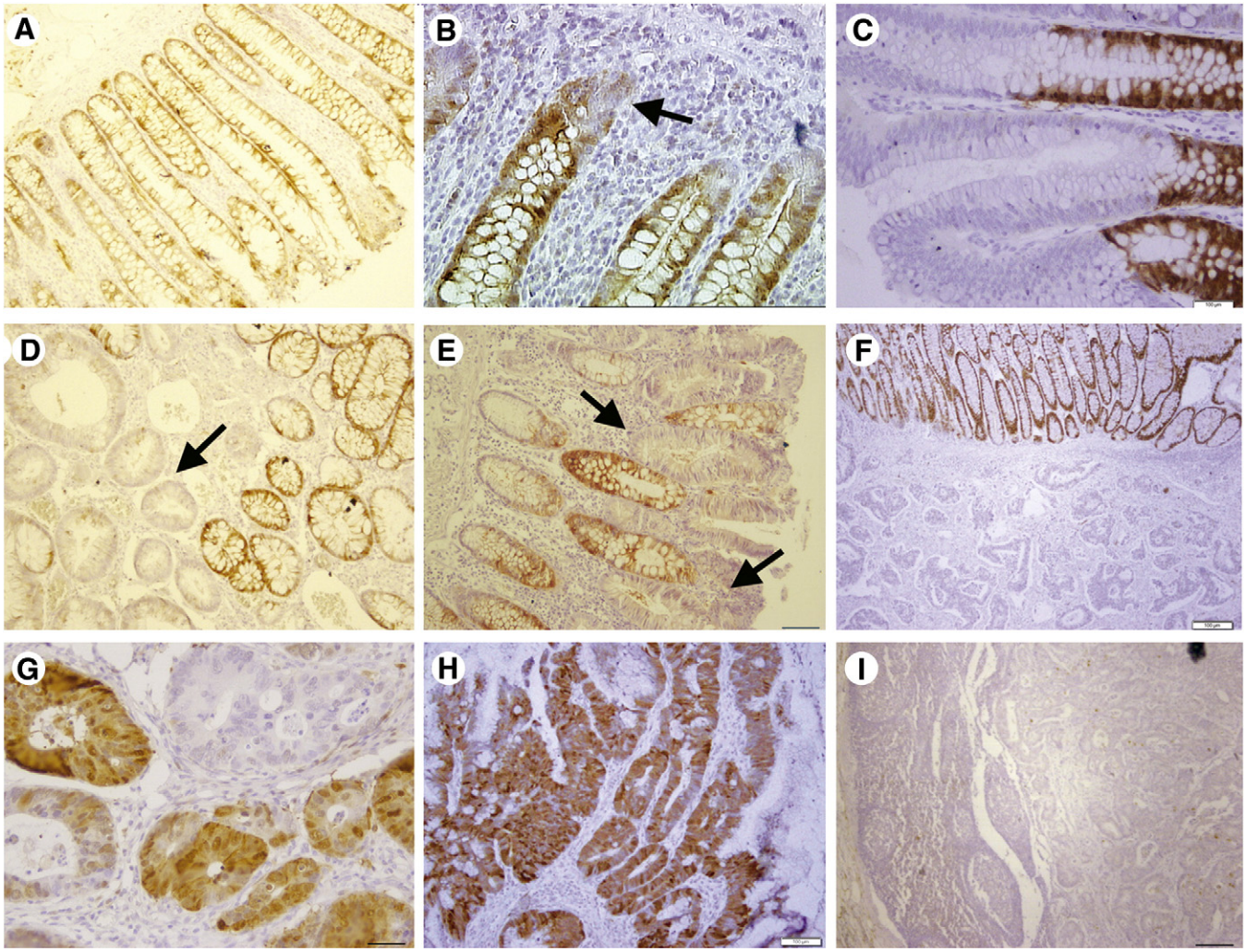

Fig. 4 IHC expression of MT1 + 2 in colorectal tissues. A, Normal colonic mucosa showing high positivity all along the crypt axis. B, Normal colonic mucosa with cells located at the bottom of the normal crypt usually stained negative (arrow). C, Representative adenoma with MT loss in the half-dysplastic fraction (left) and positive MT expression in the half normal-appearing crypts (right). D, and E, Transversal and longitudinal sections of adenomas, respectively, with normal crypts (MT-positive staining) mixed with dysplastic ones (MT-negative staining, arrows). F, Tumor tissue with totally negative MT staining (bottom) compared with highly positive adjacent normal mucosa (top). G, Carcinomatous glands showing heterogeneous positivity, as well as different subcellular localization: nuclear and cytoplasmatic. H, Tumors expressing high MT levels, usually coexist with less positive cells. I, Lymph node metastasis tissue with totally negative staining.

4. Discussion

Ever since their discovery in 1957 [14], MTs have been reported to be involved in a wide variety of cellular processes important for tumor development and progression such as proliferation, differentiation, apoptosis, angiogenesis, redox and zinc homeostasis, anti-inflammatory reactions, and immunomodulation [15,16]. Interestingly, both overexpression and underexpression of MT have been linked to poor prognosis in different tumor types [8]. In CRC, several reports have studied MT1 + 2 immunohistochemical expression, showing that MTs are heavily down-regulated in this tumor type. However, its association with patient prognosis is far from clear, with most reports showing a lack of correlation between MT and OS and DFS [17-20]. Ofner et al [21], however, report a statistically significant association of these variables with lower MT levels, whereas another study associated higher MT expression with worse prognosis, although the number of cases was low [22].

Nevertheless, what is not appreciated when assessing the tumor immunoreactivity of MT is that a family of genes (*MT1A, MT1B, MT1E, MT1F, MT1G, MT1H, MT1M, MT1X, MT2A, MT3* and *MT4*) with MT1 and MT2 being expressed ubiquitously at low levels, MT3 in neurons, glia and male reproductive organs, and MT4 in differentiating stratified squamous epithelial cells [23]. Due to the high sequence homology of MT variants, commercially available antibodies are not able to discriminate between MT1 + 2 isoforms. Therefore, studies of MT protein expression in cancer tissues include all functionally expressed isoforms.

Table 4 Histoclinical parameters of 81 cases studied

Parameter	Total no.	MT1 + 2 scores (%)			
		–	+	++	+++
Dukes stage					
A	4	25	0	50	25
B	36	31	33	28	8
C	31	39	42	16	3
D	10	60	30	10	0
pT stage [a]					
pT1	5	20	20	40	20
pT2	47	45	32	19	4
pT3	22	27	32	32	9
pT4	5	20	80	0	0
pN stage [b]					
pN0	39	31	28	31	10
pN1	27	44	48	4	4
pN2	15	40	27	33	0
M stage [c]					
M0	71	34	35	24	7
M1	10	60	30	10	0
Histologic grade					
G1	36	39	22	31	8
G2	30	40	37	20	3
G3	6	17	67	17	0
Histological type					
Nonmucinous	48	48	29	19	4
Mucinous	10	20	30	30	20
Tumor site					
Right hemicolon	36	39	39	19	3
Left hemicolon	29	28	34	31	7
Rectum	11	45	27	9	18
Tumor size (cm)					
<5	27	48	26	22	4
>5	24	38	33	17	13
Patient age (y)					
<65	20	45	30	20	5
>65	38	45	29	18	8
Patient sex					
Male	38	29	37	21	13
Female	42	45	31	24	0

[a] Tumor spread.
[b] Lymph node status.
[c] Distant metastasis.

However, due to the fact that they are variably expressed in tissues and induced by several stimuli, it is possible that different tumors express distinct MT genes, which could help explain the conflicting data on MT function in different tumor types [24]. Despite this, very few studies have specifically focused on the expression of all MT isoforms in human tumor tissues and, to our knowledge, none in CRC.

In this study, we analyzed the expression of all MT1 + 2 functional isoforms in normal and tumor tissues from 22 patients with CRC by qRT-PCR using high-grade total RNA obtained from laser capture microdissected epithelia. Our results indicated that all MTs were down-regulated in tumor tissues with respect to their normal counterparts, although at variable levels. This suggests that the expression of different isoforms is regulated by different transcription factors or mechanisms. MT1G, MT1E, and MT1F were down-regulated in 78% to 91% of cases and showed the highest reduction in mRNA levels, whereas MT1X and MT2A were lower than normal in 65% and 70% of samples, respectively, but their average down-regulation did not reach statistical significance. Interestingly, although tumors retained variable mRNA levels of MT1E, MT1M, MT1X, and MT2A, only MT1X and MT2A showed a high and significant correlation with overall MT protein levels, suggesting that these last isoforms dictate protein expression and therefore MT functionality in CRC.

Remarkably, similar results have been obtained in breast, thyroid, renal, prostate, and bladder cancer [25-29], showing that MT2A and MT1X expression was always consistent with the level of MT1 + 2 protein up-regulation or down-regulation in these tumors, whereas MT1G, MT1A, MT1E, and MT1F were down-regulated, irrespective of protein expression.

CRC cell lines showed a similar pattern of MT expression to tumor tissues, in that they mainly expressed MT1E, MT1X, and MT2A isoforms, at variable levels and with different subcellular localization of MT protein. Given that all cell lines are grown in the same culture media and therefore with the same Zn^{2+} concentrations, this suggests that their heterogeneity in MT expression is due to intrinsic characteristics of the tumors and not to environmental factors.

Next, we demonstrated that the *MT1G* promoter was hypermethylated in 4 (29%) of 14 of tumors studied and in 2 of 5 CRC cell lines. The functional significance of the methylation levels obtained from MSP analysis was confirmed by the induction of MT1G mRNA expression after DAC treatment of cell lines. This does not necessarily imply that the same would hold true in the in vivo setting, but if this were the case, a plausible mechanism for MT1G reinduction in patients would be suggested. Importantly, some colorectal tissues and cell lines with *MT1G* promoter hypermethylation presented high levels of MT1 + 2 protein and MT1X and MT2A mRNA, further supporting the idea that these isoforms are regulated differently. *MT1G* hypermethylation has also been found in other tumor types and has been associated with higher tumor aggressiveness [30-37]. DAC treatment analysis further suggested that *MT1H* and *MT1A* might also be regulated by promoter hypermethylation. Because most tumors presented MT1G down-regulation but only 29% were methylated, further mechanisms should account for MT1G repression in these tumors. We found that MTs can be regulated by other epigenetic mechanisms involving HDACs because HDAC inhibitor treatment induced the expression of most isoforms. These results could have important therapeutic consequences because patients with CRC could therefore benefit from demethylating or HDAC inhibitor treatments.

We then analyzed MT1 + 2 IHC expression in colorectal normal mucosae, adenomas, carcinomas, and lymph node metastases. Most normal-appearing mucosae (both from nononcologic patients and from patients with CRC) showed high expression of MTs. We observed that cells at the very base

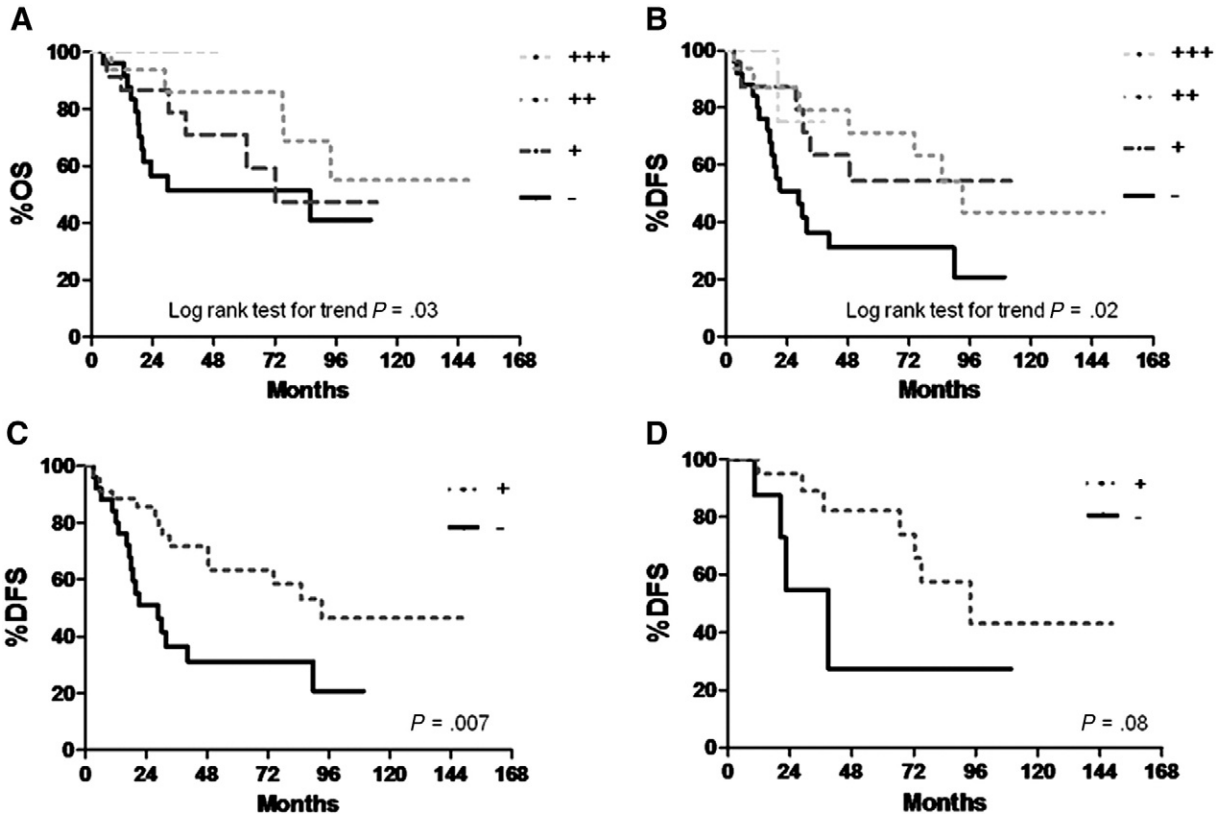

Fig. 5 Kaplan-Meier survival curves. MT positivity was inversely associated with shorter OS (A) and DFS (B). C, Totally negative scores showed a significantly worse DFS (log-rank test, $P = .007$). D, When analyzing only Dukes B cases, totally negative cases showed a trend in association with worse DFS ($P = .08$).

of the crypt were often negative for MT staining, which is particularly important because intestinal stem cells are supposed to be located at the lower basal layers of the crypt [38]. Furthermore, in agreement with other studies [6,7,39], we showed that MT down-regulation is an early step in CRC progression, already evident in low- and high-grade adenomas. Whether this alteration is a necessary step for tumor development or an accompanying feature is an important question that remains to be elucidated. However, support for the first possibility comes from studies that show that MT knockout mice are more susceptible to chemically induced carcinogenesis than wild-type animals [40,41].

MT1 + 2 expression was down-regulated in 94% (76/81) of carcinomas, with increasing MT positivity leading to progressively better survival. Patients with completely negative tumors (37% of total) had a significantly worse OS and DFS than did patients with positive tumors. Interestingly, when analyzing Dukes stages individually, negative MT staining showed a nonsignificant trend in association with shorter DFS in Dukes B but not in Dukes C cases. Despite this, the high HR obtained (3.8) makes it particularly interesting to study this situation in further detail because the benefit of adjuvant chemotherapy in these patients (40% of resected cancers) is controversial due to the small gains in survival [42]. Therefore, discovery of new biomarkers that may subdivide Dukes B patients into more defined prognostic categories may be of importance to facilitate treatment decisions. In multivariate analysis, only Dukes stage and mucinous histology were independent predictors of survival. Furthermore, no correlation could be established between MT staining and routine histoclinical parameters. This survival analysis suggests that although MT loss is an early event in tumor progression and is therefore a common feature of CRC tumors, it might still prove

Table 5 Univariate survival analysis: log-rank test

Parameter	OS			DFS		
	χ^2	*df*	*P*	χ^2	*df*	*P*
Dukes stage [a]	11.90	1	.0006	10.77	1	.0010
pT stage	12.28	3	.0065	8.57	3	.0356
pN stage	7.36	2	.0252	8.35	2	.0153
M stage	12.84	1	.0003	10.28	1	.0013
MT [a]	4.51	1	.0337	5.16	1	.0231
Tumor site	5.72	2	NS	1.37	2	NS
Histologic type	2.90	1	NS	7.93	1	.0049
Histologic grade	0.27	2	NS	0.39	2	NS
Tumor size	0.22	1	NS	1.46	1	NS
Patient age	0.14	1	NS	0.07	1	NS
Patient sex	0.07	1	NS	0.99	1	NS

Abbreviation: *df*, degrees of freedom.
[a] Log-rank test for trend.

to be a useful prognostic biomarker. This needs to be confirmed in larger independent data sets. We suggest that this may be due to a subset of isoforms (MT1X and/or 2A), and thus, their measurement might improve the prognostic ability of MTs.

In conclusion and taking into account all of the above results, we suggest a model in which the early loss of MT protein expression along the adenoma-carcinoma sequence would mainly be due to MT1G, MT1F, and/or MT1E down-regulation, because their mRNA levels are significantly reduced in most tumors. Of the remaining isoforms, only MT1X and MT2A would dictate protein expression in tumors. Some of these tumors would further repress these isoforms as well and thus contribute to worse patient prognosis. These MT expression changes may be brought about by epigenetic mechanisms such as the promoter hypermethylation of specific isoforms or HDAC-mediated repression of most MTs. In light of the known free radical scavenging and detoxifying properties of MTs, we speculate that they may act as protective agents for normal colonic epithelium against potentially tumorigenic stimuli present in the intestinal environment. Their down-regulation might thus facilitate tumor development and progression.

This study provides evidence for studying in further detail the functional significance of the down-regulation of different isoforms for CRC progression and the possibility that MT reinduction (using demethylating or HDAC inhibitor agents) could be used for CRC therapy.

Supplementary materials related to this article can be found online at doi:10.1016/j.humpath.2011.04.015.

References

[1] West AK, Stallings R, Hildebrand CE, Chiu R, Karin M, Richards RI. Human metallothionein genes: structure of the functional locus at 16q13. Genomics 1990;8:513-8.

[2] Bell SG, Vallee BL. The metallothionein/thionein system: an oxidoreductive metabolic zinc link. Chembiochem 2009;10:55-62.

[3] Klaassen CD, Liu J, Diwan BA. Metallothionein protection of cadmium toxicity. Toxicol Appl Pharmacol 2009;238:215-20.

[4] Udom AO, Brady FO. Reactivation in vitro of zinc-requiring apo-enzymes by rat liver zinc-thionein. Biochem J 1980;187:329-35.

[5] Zeng J, Heuchel R, Schaffner W, Kägi JH. Thionein (apometallothionein) can modulate DNA binding and transcription activation by zinc finger containing factor Sp1. FEBS Lett 1991;279:310-2.

[6] Janssen AM, van Duijn W, Oostendorp-Van De Ruit MM, et al. Metallothionein in human gastrointestinal cancer. J Pathol 2000;192:293-300.

[7] Mulder TP, Verspaget HW, Janssens AR, de Bruin PA, Griffioen G, Lamers CB. Neoplasia-related changes of two copper (Cu)/zinc (Zn) proteins in the human colon. Free Radic Biol Med 1990;9:501-6.

[8] Pedersen M, Larsen A, Stoltenberg M, Penkowa M. The role of metallothionein in oncogenesis and cancer prognosis. Prog Histochem Cytochem 2009;44:29-64.

[9] Notterman DA, Alon U, Sierk AJ, Levine AJ. Transcriptional gene expression profiles of colorectal adenoma, adenocarcinoma, and normal tissue examined by oligonucleotide arrays. Cancer Res 2001;61:3124-30.

[10] Türeci O, Ding J, Hilton H, et al. Computational dissection of tissue contamination for identification of colon cancer-specific expression profiles. FASEB J 2003;17:376-85.

[11] Bianchini M, Levy E, Zucchini C, et al. Comparative study of gene expression by cDNA microarray in human colorectal cancer tissues and normal mucosa. Int J Oncol 2006;29:83-94.

[12] Herman JG, Graff JR, Myöhänen S, Nelkin BD, Baylin SB. Methylation-specific PCR: a novel PCR assay for methylation status of CpG islands. Proc Natl Acad Sci USA 1996;93:9821-6.

[13] Remmele W, Stegner HE. Vorschlag zur eincheitlichen Definition eines Immunoreaktiven Score (IRS) für den immunohistochemischen Ostrogenrezeptor-Nachweis (ER-ICA) im Mammakarzinomgewebe. Der Pathologe 1987;8:138-40.

[14] Margoshes M, Vallee BL. A cadmium protein from equine kidney cortex. J Am Chem Soc 1957;79:4813-4.

[15] Dutsch-Wicherek M, Sikora J, Tomaszewska R. The possible biological role of metallothionein in apoptosis. Front Biosci 2008;13:4029-38.

[16] Nielsen AE, Bohr A, Penkowa M. The balance between life and death of cells: roles of metallothioneins. Biomark Insights 2006;1:99-111.

[17] Sutoh I, Kohno H, Nakashima Y, et al. Concurrent expressions of metallothionein, glutathione *S*-transferase-pi and *P*-glycoprotein in colorectal cancers. Dis Colon Rectum 2000;43:221-32.

[18] Schmitz KJ, Müller CI, Reis H, et al. Combined analysis of hypoxia-inducible factor 1 alpha and metallothionein indicates an aggressive subtype of colorectal carcinoma. Int J Colorectal Dis 2009;24:1287-96.

[19] Dziegiel P, Forgacz J, Suder E, Surowiak P, Kornafel J, Zabel M. Prognostic significance of metallothionein expression in correlation with Ki-67 expression in adenocarcinomas of large intestine. Histol Histopathol 2003;18:401-7.

[20] Bouzourene H, Chaubert P, Gebhard S, Bosman FT, Coucke P. Role of metallothioneins in irradiated human rectal carcinoma. Cancer 2002;95:1003-8.

[21] Ofner D, Maier H, Riedmann B, et al. Immunohistochemical metallothionein expression in colorectal adenocarcinoma: correlation with tumour stage and patient survival. Virchows Archiv 1994;425:491-7.

[22] Hishikawa Y, Kohno H, Ueda S, et al. Expression of metallothionein in colorectal cancers and synchronous liver metastases. Oncology 2001;61:162-7.

[23] Laukens D, Waeytens A, De Bleser P, Cuvelier C, De Vos M. Human metallothionein expression under normal and pathological conditions: mechanisms of gene regulation based on in silico promoter analysis. Crit Rev Eukaryot Gene Expr 2009;19:301-17.

[24] Jasani B, Schmid KW. Significance of metallothionein overexpression in human tumours. Histopathology 1997;31:211-4.

[25] Jin R, Chow VT, Tan PH, Dheen ST, Duan W, Bay BH. Metallothionein 2A expression is associated with cell proliferation in breast cancer. Carcinogenesis 2002;23:81-6.

[26] Ferrario C, Lavagni P, Gariboldi M, et al. Metallothionein 1G acts as an oncosupressor in papillary thyroid carcinoma. Lab Invest 2008;88:474-81.

[27] Nguyen A, Jing Z, Mahoney PS, et al. In vivo gene expression profile analysis of metallothionein in renal cell carcinoma. Cancer Lett 2000;160:133-40.

[28] Garrett SH, Sens MA, Shukla D, et al. Metallothionein isoform 1 and 2 gene expression in the human prostate: downregulation of MT-1X in advanced prostate cancer. Prostate 2000;43:125-35.

[29] Somji S, Sens MA, Lamm DL, Garrett SH, Sens DA. Metallothionein isoform 1 and 2 gene expression in the human bladder: evidence for upregulation of MT-1X mRNA in bladder cancer. Cancer Detect Prev 2001;25:62-75.

[30] Sakamoto LH, DE Camargo B, Cajaiba M, Soares FA, Vettore AL. MT1G hypermethylation: a potential prognostic marker for hepatoblastoma. Pediatr Res 2010;67:387-93.

[31] Henrique R, Jerónimo C, Hoque MO, et al. MT1G hypermethylation is associated with higher tumor stage in prostate cancer. Cancer Epidemiol Biomarkers Prev 2005;14:1274-8.
[32] Kang GH, Lee S, Cho NY, et al. DNA methylation profiles of gastric carcinoma characterized by quantitative DNA methylation analysis. Lab Invest 2008;88:161-70.
[33] Huang Y, de la Chapelle A, Pellegata NS. Hypermethylation, but not LOH, is associated with the low expression of MT1G and CRABP1 in papillary thyroid carcinoma. Int J Cancer 2003;104:735-44.
[34] Kanda M, Nomoto S, Okamura Y, et al. Detection of metallothionein 1G as a methylated tumor suppressor gene in human hepatocellular carcinoma using a novel method of double combination array analysis. Int J Oncol 2009;35:477-83.
[35] Koga Y, Pelizzola M, Cheng E, et al. Genome-wide screen of promoter methylation identifies novel markers in melanoma. Genome Res 2009;19:1462-70.
[36] Tokumaru Y, Yamashita K, Osada M, et al. Inverse correlation between cyclin A1 hypermethylation and p53 mutation in head and neck cancer identified by reversal of epigenetic silencing. Cancer Res 2004;64:5982-7.
[37] Adams L, Roth MJ, Abnet CC, et al. Promoter methylation in cytology specimens as an early detection marker for esophageal squamous dysplasia and early esophageal squamous cell carcinoma. Cancer Prev Res (Phila Pa) 2008;1:357-61.
[38] McDonald SA, Preston SL, Lovell MJ, Wright NA, Jankowski JA. Mechanisms of disease: from stem cells to colorectal cancer. Nat Clin Pract Gastroenterol Hepatol 2006;3:267-74.
[39] Kuroda K, Aoyama N, Tamura T, Sakashita M, Maekawa S, Inoue T. Variation in MT expression in early-stage depressed-type and polypoid-type colorectal tumours. Eur J Cancer 2002;38:1879-87.
[40] Majumder S, Roy S, Kaffenberger T, et al. Loss of metallothionein predisposes mice to diethylnitrosamine-induced hepatocarcinogenesis by activating NF-{kappa}B target genes. Cancer Res 2010;70:10265-76.
[41] Suzuki JS, Nishimura N, Zhang B, et al. Metallothionein deficiency enhances skin carcinogenesis induced by 7,12-dimethylbenz[*a*]anthracene and 12-*O*-tetradecanoylphorbol-13-acetate in metallothionein-null mice. Carcinogenesis 2003;24:1123-32.
[42] Cunningham D, Starling N. Adjuvant chemotherapy of colorectal cancer. Lancet 2007;370:1980-1.